JOURNAL OF MATERIALS SCIENCE 35 (2000) 1187–1193

Mechanical properties and fracture morphologies of poly(phenylene sulfide)/nylon66 blends—effect of nylon66 content and testing temperature

SANG IL LEE, BYOUNG CHUL CHUN
Department of Polymer Engineering, College of Engineering, The University of Suwon, Hwasung-gun, Kyonggi-do, Korea
E-mail: bcchun@mail.suwon.ac.kr

Poly(phenylene sulfide) (PPS) was melt blended with Nylon66 and the mechanical properties and corresponding fracture morphologies were investigated. The thermal distortion temperature (HDT) of PPS/Nylon 66 blend showed that the inherent thermal stability of pure PPS can be maintained up to 30 wt% Nylon66, but then it started to decrease linearly thereafter to that of pure Nylon66 based on the rule of mixtures relationship. Tensile tests of PPS/Nylon66 blends at testing temperatures of −30, 25, 75, and 150°C showed that the maximum stress decreased up to 30 wt% Nylon66, and started to increase thereafter. Strain at break showed little change at low nylon content regardless of testing temperature, however, a large strain at break increase could be observed at more than 30 wt% Nylon66 and at 150°C testing temperature. At the same testing temperatures, the impact strength of PPS/Nylon66 blends was investigated, and it was found that an impact strength increase at all testing temperatures could be observed at more than 30 wt% Nylon66.

1. Introduction

Poly(phenylene sulfide) (PPS) was first commercialized by Philips Petroleum Co. in 1973. PPS has a glass transition temperature of 80–90°C and melting temperature of 280°C. PPS has good dimensional stability, high strength, high modulus, chemical and fatigue resistance, and can be a metal substitute engineering plastic. PPS is synthesized from p-dichlorobenzene and sodium sulfide in an organic solvent. However, PPS has brittle nature, low strain at break and slow crystallization rate, thus it is generally used as a glass fiber reinforced composite form. Regarding these weaknesses, there have been papers on the crystal structure [1–3], rheological properties in a melt state [4–8], and melt crystallization behavior [9–13]. Also, there are papers on the carbon, glass and aramid fiber reinforced PPS composites [14–18], PPS/thermoplastic polymer blends [19–23], and PPS/liquid crystal polymer blends [24–26]. These papers generally deal with the method of improving the brittle nature and low strain at break of PPS by analyzing the rheological properties, crystallization behavior and mechanical fracture morphologies, however, systematic studies on the interrelationships between these characteristics are still in its early stages. Moreover, studies on the PPS blends are limited to the blends with general-purpose plastics such as polyethylene (PE). Thus, in this investigation, Nylon66 with high toughness and chemical resistance was blended with PPS. Their mechanical properties and corresponding fracture morphologies were studied at various Nylon66 contents and testing temperatures, and a possibility of finding a new PPS/Nylon66 blend which can maintain the inherent high mechanical properties of PPS as well as impact strength and toughness of Nylon66 was pursued.

2. Experimental procedure

2.1. Materials

PPS used in this investigation is a commercial SUNTRA S-500 grade (Mw = 30,000 g/mol) produced by SK Chemicals, and Nylon66 was Zytel 101L grade produced by Du Pont. Zytel 101L has a glass transition temperature of 50–60°C and a melting temperature of 250°C. PPS and Nylon66 was melt blended using twin screw compounder (Toshiba, co-rotating intermeshing type, $\phi = 35$ mm), and Nylon66 content was set to 0, 10, 20, 30, 50, 70, 100 wt%, respectively. Screw speed was 350 rpm and processing temperature was 315–320°C. Specimens for mechanical property tests were injection molded using Engel ES240/75P injection molder according to the ASTM specifications. Mold temperature was 150°C, cylinder temperature was 285–295°C, and screw speed was 157–160 rpm. All specimens were annealed at 50°C for 24 hrs to remove any residual stress in an oven before the test.

2.2. Heat distortion temperature (HDT) measurement

HDT was measured according to ASTM D648 using an ATS Farr (HDT-VICAT tester MP/3). At least 5

specimens were tested and the average value was used for the data plot.

2.3. Tensile test

Tensile testing was performed using Lloyd Instrument (LR 50K). ASTM D638 type specimens were used, and the crosshead speed was 50 mm/min and gauge length was 100 mm. Tensile tests were performed at four different temperatures (−30, 25, 75, 150°C) in order to evaluate the effect of testing temperature change with respect to the glass transition temperatures of the blend components. All tests were conducted in an environmental chamber with a storage time of at least 1 hr. To evaluate the effect of storage time on the mechanical properties, specimens were stored up to 10 hrs, however, test results were the same after 1 hr storage time. A minimum 5 specimens for each blend composition were tested and the average value was used for the data plot.

2.4. Notched Izod impact strength

At least 10 specimens were used according to ASTM D256 specification, and tests were performed using Testing Machines Inc. (model 43-02) impact tester. Identical testing temperatures were used as in the tensile tests, and the sample storage time was set to 1 hr.

2.5. Morphological observation

In order to observe the fracture surface morphology change from the tensile and impact tests as well as composition change, a scanning electron microscope (JEOL, JSM-5200) was employed and the operating voltage was set to 20 kV. For the observation of dispersed particle size and size distribution, specimens were fractured under the liquid nitrogen condition, and the fracture surface was observed with the SEM. These SEM photomicrographs were scanned with scanner (HP ScanJet 4p), and the scanned images were analyzed using Image Pro Plus for windows v.1.2 by Media Cybernetics. First, several zones were selected from the scanned image, and the dispersed particles from each zone (more than one hundred particle size) were analyzed using the above program and from this the average particle size and standard deviation were determined. In order to compare the dispersed particles of blends with different compositions, all specimens were treated with an identical processing condition.

3. Results and discussion

3.1. Phase morphology observation

Fig. 1 shows the dispersed particle size and distribution of PPS/Nylon66 blends before and after the phase inversion. When Nylon66 is a dispersed phase, the particle size increases as the Nylon66 content increases. Generally, the particle size was around 0.13–0.15 μm and size distribution was narrow up to 20 wt% Nylon66, however, at 30 wt% Nylon66, the particle size and distribution increased about twofold compared to 10 wt% Nylon66, and the particle size was around 0.25 μm.

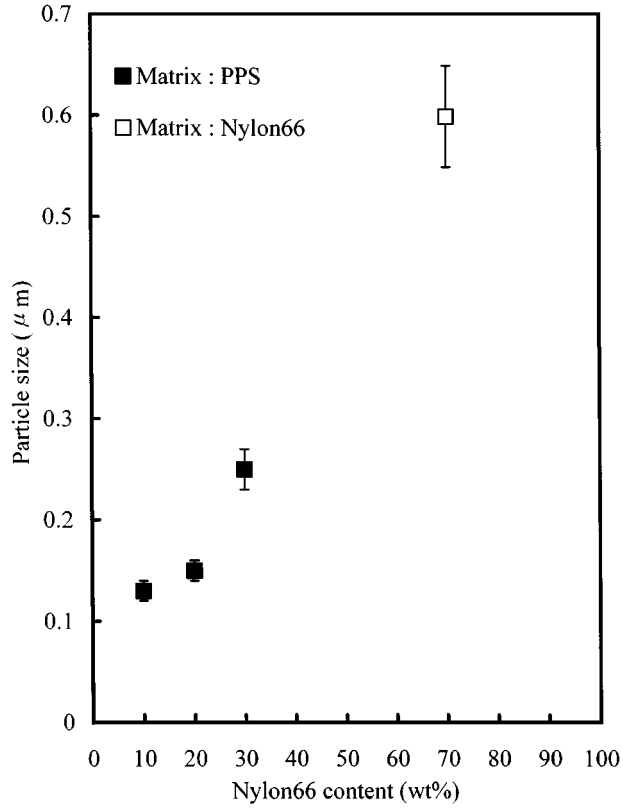

Figure 1 Average particle size and size distribution (Bar indicates 95% confidence limit).

According to Chen and Su [19] who studied the morphology of PPS/polyethylene (PE) blends, more elastic particles tend to increase the interfacial tension within a relatively low elastic matrix, thus it becomes more stable to the applied deformation and results in an uneven distribution of particles. Thus, as the dispersed phase content increases, the distance between the dispersed particles becomes reduced and leads to the coalescence of dispersed particles. In other words, these authors stated that dispersed PE was more elastic compared to the PPS matrix, and as the PE content increased PE became less well dispersed and led to the increase of PE particle size. When PPS is a dispersed phase, there should be no change in PPS particle size. However, in their investigation, viscoelastic theory could be applied to the particle size increase when PE was a dispersed phase, but when PPS was a dispersed phase, there was not enough analysis for the PPS particle size and size increase.

In this investigation, the Nylon66 particle size and distribution increase phenomenon with increasing Nylon66 content can be explained using the above mentioned relative differences in elasticity. Also it can be explained that Nylon66 dispersion is severely limited within the higher melt viscosity PPS matrix. This particle size and distribution increase was clearly observed at 30 wt% Nylon66.

3.2. Heat distortion temperature (HDT) measurement

Fig. 2 shows the HDT results of PPS/Nylon66 blends. As can be seen, PPS/Nylon66 blends with up to 30 wt%

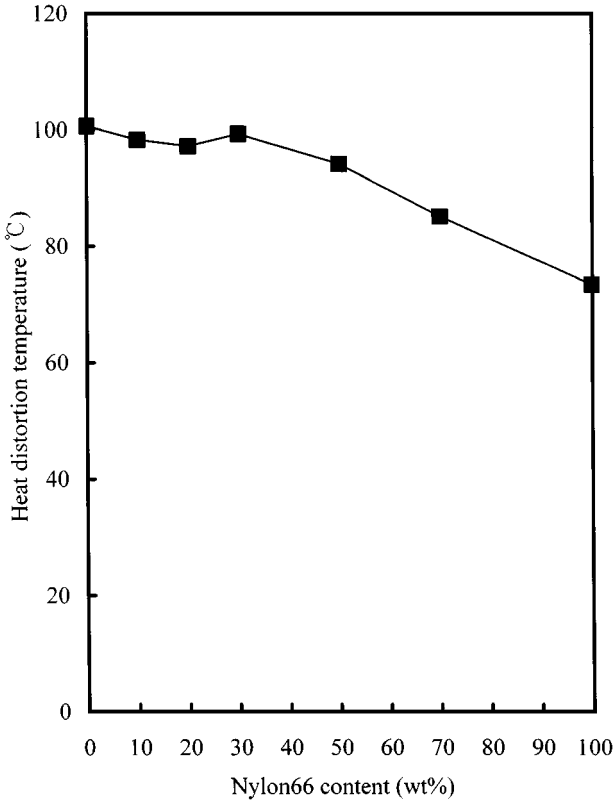

Figure 2 Heat distortion temperature vs. Nylon66 content of PPS/Nylon66 blends.

Nylon66 have HDTs similar to pure PPS (100.7°C), however, at more than 30 wt% Nylon66, the HDT decreases linearly to that of pure Nylon66 (73.7°C). Cheung *et al.* [21] who studied the thermal behavior and morphology of PPS/polysulfone (PSF) blends insisted that when the component with lower glass transition temperature was a dispersed phase (less than 50 vol%), then the HDT of the blend was not affected by the dispersed phase. Thus, when Nylon66 which has lower glass transition temperature compared to PPS is a dispersed phase (up to 30 wt% Nylon66), the blend can maintain the HDT of pure PPS. This enables the PPS/Nylon66 blend up to the phase inversion point to retain the high temperature dimensional stability of pure PPS regardless of dispersed particle size, distribution, dispersion mode and interfacial bonding.

However, in the opposite case such as the component with higher glass transition temperature as the dispersed phase, then the HDT behavior of the blend follows the rule of mixtures relationship, with either positive or negative deviation from this rule. In our investigation, when PPS is the dispersed phase, the HDT shows a linear decrease. From these results, when PPS is the dispersed phase, as Jog and Nadkarni indicated in their study on the PPS/polyethylene terephthalate (PET) blend [13], there occur interactions between the constituents. In this case, the word interaction means that, in the melt crystallization process, a fast-solidified dispersed particle can act as a nucleus to the matrix that is still in the melt state. From the molecular point of view, Nylon66 matrix chains can start the crystallization process around the already solidified PPS particles and result in an increase of interfacial bonding. Thus, in this investigation, the reason for the observed increased interfacial bonding when PPS is the dispersed phase is due to the nucleating agent role of fast-solidified PPS particles within the Nylon66 matrix.

3.3. Tensile test and fracture surface observation

Fig. 3 shows the maximum stress of PPS/Nylon66 blends. Generally, maximum stress decreased up to 20 wt% Nylon66, and started to increase thereafter to that of pure Nylon66. And the tensile behavior with respect to the testing temperature change shows two distinctive behaviors depending on the glass transition temperatures of constituents PPS and Nylon66. Below the glass transition temperature of PPS and Nylon66 such as −30 and 25°C testing condition, tensile behavior is almost the same. However, at 75 and 150°C testing condition, tensile properties indicate that this behavior is due to the thermal deformation characteristics of Nylon66 and PPS at above their glass transition temperatures. Also with regard to 30 wt% Nylon66, it shows a brittle fracture nature up to 20 wt% Nylon66, and ductile fracture at more than 30 wt% Nylon66. These are in good agreement with the strain at break results shown in Fig. 4, and especially, the strain at break change was large at 75 and 150°C testing conditions.

Fig. 5 shows the tensile fractured surface morphology of PPS/Nylon66 blend. Fig. 5a shows the tensile fractured surface of pure PPS at 150°C testing condition. As can be seen, even though the testing temperature is higher than the HDT of pure PPS (100.7°C), the fracture surface is more like a glass fracture surface rather

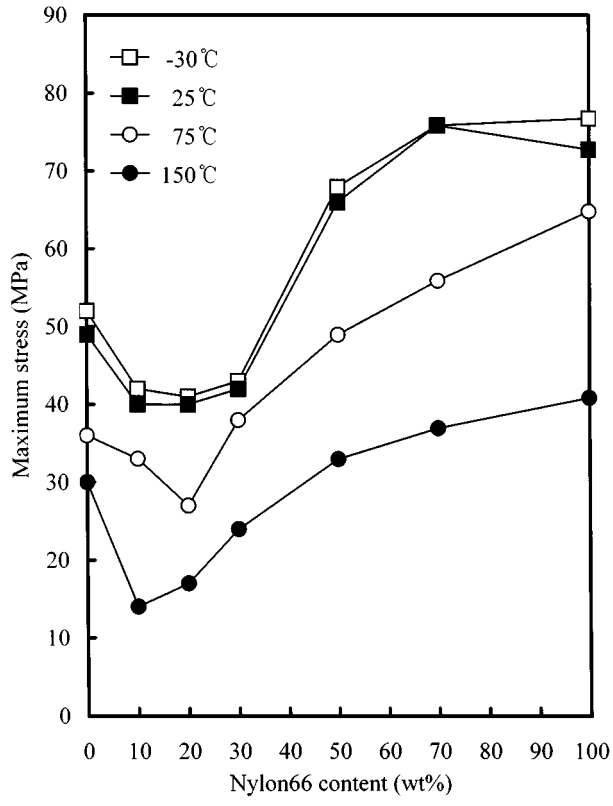

Figure 3 Maximum stress vs. Nylon66 content of PPS/Nylon66 blends at various testing temperatures.

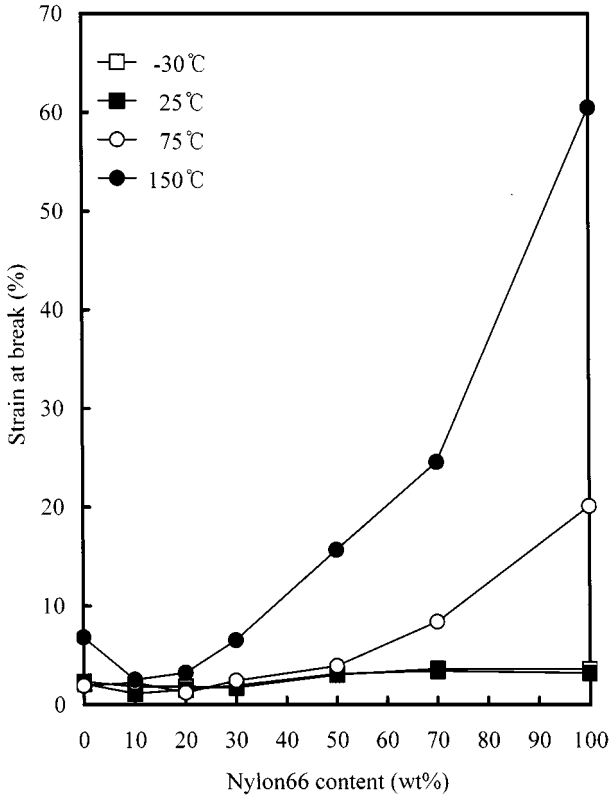

Figure 4 Strain at break vs. Nylon66 content of PPS/Nylon66 blends at various testing temperatures.

than ductile fracture morphology which can be deduced from the sharp crack propagation path.

In contrast, when Nylon66 is the dispersed phase (20 wt% Nylon66), the dispersed particle in the fracture surface is not observed even though there is a testing temperature change as shown in Fig. 5b and c, and this indicates that the effective fracture energy dispersion is difficult. From this observation it can be concluded that the fracture energy dispersion during the tensile test occurs at the weak interface between PPS and Nylon66, and brittle PPS deformation. Fig. 5b shows the tensile fractured surface morphology of dispersed PPS tested at 150°C. At this temperature, with the softening of matrix Nylon66, as was already discussed in the HDT results, PPS particles can be found remaining in the matrix due to the increased interfacial bonding resulting from the nucleus role of PPS within the Nylon66 matrix.

Fig. 6 shows the modulus of elasticity of PPS/Nylon66 blends. As in the case of HDT results, the modulus of elasticity linearly decreased with increasing Nylon66. At −30, 25 and 150°C testing condition, the modulus of elasticity change is not great, however, at 75°C testing condition, the modulus of elasticity decrease was profound. This is due to the fact that at 75°C testing condition, pure PPS retains high modulus, whereas, Nylon66 has lower modulus because it is above its glass transition temperature. Generally,

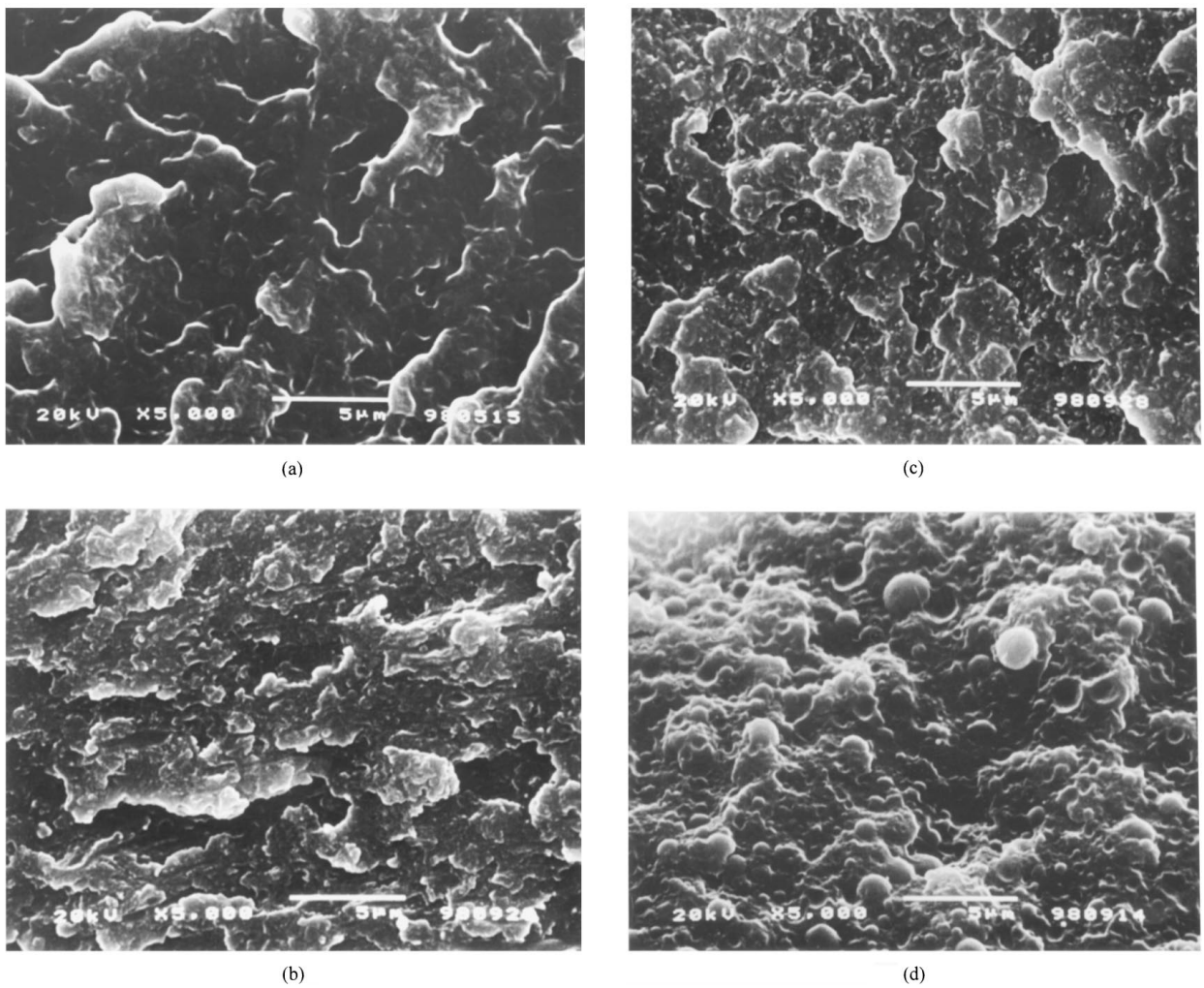

Figure 5 SEM photomicrographs of tensile fractured surfaces of (a) pure PPS at 150°C, (b) 80 wt%/PPS/20 wt% Nylon66 blend at 25°C, (c) 80 wt%/PPS/20 wt% Nylon66 blend at 150°C, (d) 30 wt%PPS/70 wt% Nylon66 blend at 150°C.

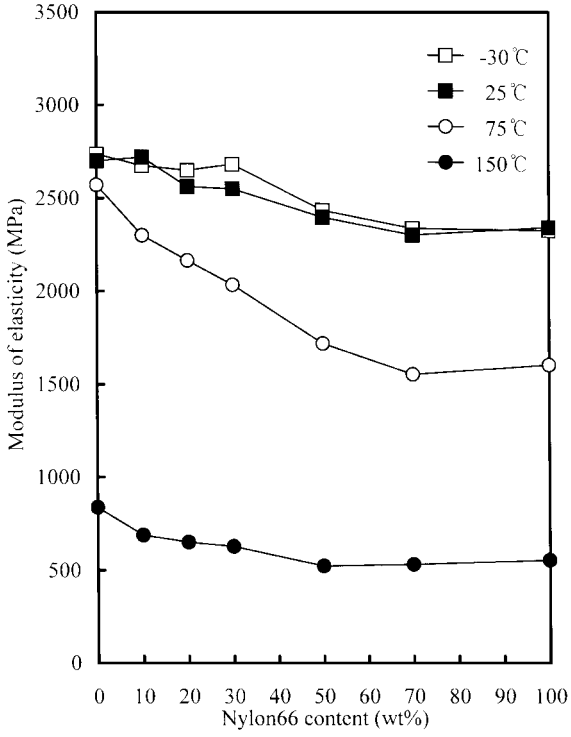

Figure 6 Modulus of elasticity vs. Nylon66 content of PPS/Nylon66 blends at various testing temperatures.

blending with other polymers results in a modulus change depending on the composition, however, as can be observed from this analysis, it can be concluded that modulus change of PPS/Nylon66 blend is not greatly affected by Nylon66 content increase.

3.4. Notched Izod impact test and fracture surface observation

Fig. 7 shows Izod impact test results with Nylon66 content and test temperature change. Generally, as in HDT and tensile tests, the impact strength did not change much up to 30 wt% Nylon66. However, at more than this content, in other words, at above its phase inversion content, impact strength increased regardless of test temperature. Especially at 150°C, impact strength increased dramatically. Generally, when the deformation occurs by external stress, fracture energy dispersion can be absorbed at the matrix, the dispersed phase, and the interface between matrix and dispersed phase. Thus, external stress can be dispersed in a variety of ways such as matrix plastic deformation, interfacial separation between matrix and dispersed phase, craze pinning by the dispersed phase, and even fracture of the dispersed phase itself. In a polymer blend, this type of effective energy dispersion can be greatly affected by the interfacial bonding between the dispersed phase and matrix.

Fig. 8 shows the impact fractured surface of PPS/Nylon66 blend. Fig. 8a and b show the impact fractured surface when 30 wt% Nylon66 is a dispersed phase, and Fig. 8c and d show the impact fractured surface when 30 wt% PPS is a dispersed phase at −30 and 150°C, respectively. As can be seen in Fig. 8a, the matrix fracture surface is a typical PPS brittle fracture and is like a glass fracture, and also from the observation of interfacial bonding state of dispersed Nylon66 particles, it can be easily concluded that the bonding force is not good. However, this brittle matrix fracture characteristic is slightly improved as can be known from the observation of fracture morphology shown in Fig. 8b tested at 150°C. However, even though there occurs matrix wetting by PPS plastic deformation and Nylon66 softening, from the observation of clear protrusion of dispersed particles and almost sphere like fracture morphology, it can be concluded that this is not good enough to improve the low impact resistance.

Meanwhile, the matrix deformation state and particle dispersion type as shown in Fig. 8c and d is quite different from the morphology shown in Fig. 8a and b. When Nylon66 is the matrix, the fracture characteristic at −30°C testing condition includes the rough morphology and partially exposed dispersed particles, which indicate matrix ductility. The reason for this is the increased interfacial bonding resulting from the nucleating role of PPS particles by different crystallization behavior already mentioned in the HDT discussion. Even though the matrix ductility is good, if there is a weak interfacial bonding, then the dispersed PPS particles will protrude and offer a crack propagation path as the crack grows and result in a fracture characteristic which moves along the densely populated PPS regions. However, as indicated from the observation of particle size, PPS has bigger particle size and irregular distribution than when the Nylon66 is the dispersed phase. And the fact that it exhibits high impact strength indicates that this is due to the increased interfacial adhesion by the nucleating agent role of PPS. Even though occasional separation of PPS particles is observed, overall morphology characteristics are like

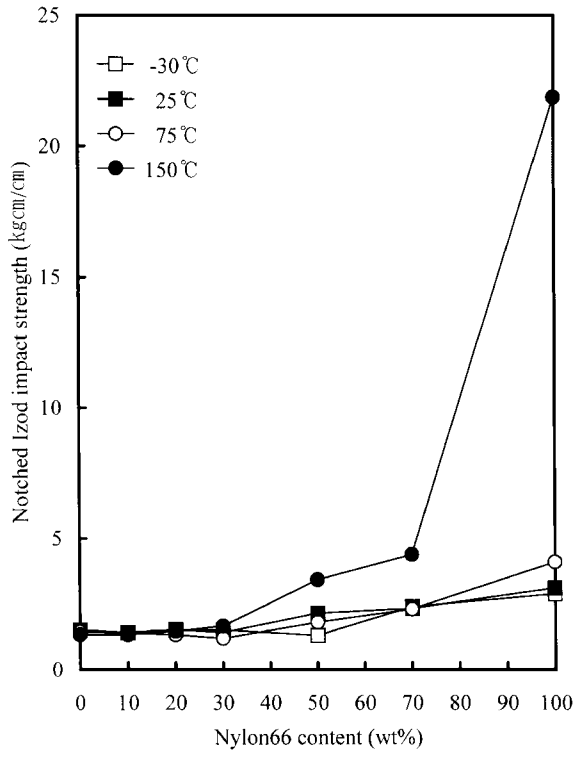

Figure 7 Notched Izod impact strength vs. Nylon66 content of PPS/Nylon66 blends at various testing temperatures.

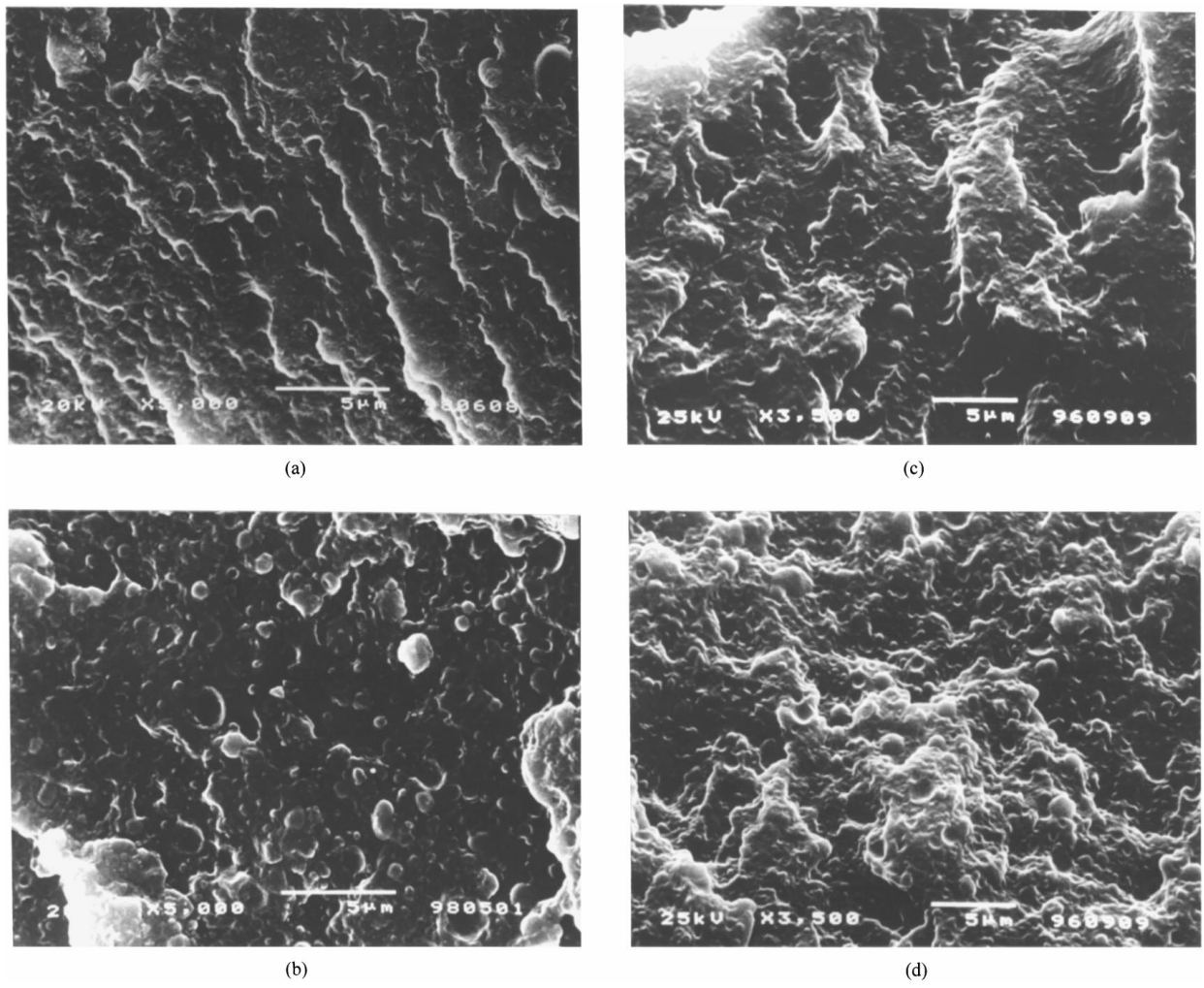

Figure 8 SEM photomicrographs of impact fractured surfaces of (a) 70 wt%/PPS/30 wt% Nylon66 blend at −30°C, (b) 70 wt% PPS/30 wt%Nylon66 blend at 150°C, (c) 30 wt%/PPS/70 wt% Nylon66 blend at −30°C, (d) 30 wt% PPS/70 wt% Nylon66 blend at 150°C.

softened Nylon66 matrix covering the PPS dispersed particles. Thus, the high impact strength at 150°C is due to the proper interfacial bonding between PPS and Nylon66 as well as Nylon66 plastic deformation resulting from the high temperature test condition.

4. Conclusion

HDT change of PPS/Nylon66 blend with increasing Nylon66 showed that the blend maintained the thermal stability of pure PPS up to the phase inversion, then showed a rule of mixtures relationship decrease thereafter. Tensile tests of PPS/Nylon66 blends at the testing temperatures of −30, 25, 75 and 150°C showed that a maximum stress and strain at break increase was observed at more than 30 wt% Nylon66. The modulus of elasticity showed a rather linear decrease. The Notched Izod impact strength at the same testing temperatures showed that impact strength increased as in a tensile test at more than 30 wt% Nylon66. Also, when PPS was a dispersed phase, it showed an excellent interfacial bonding compared to the opposite case, and due to this improved bonding, rather increased mechanical properties could be observed.

Acknowledgements

Financial support from the KOSEF (981-1107-036-2) is gratefully acknowledged.

References

1. J. ANDREW, F. LOVINGER, J. PADDEN JR. and D. DAVIS, *Polymer* **29** (1988) 229.
2. L. DLARIO and A. PIOZZI, *J. Mater. Sci. Letters* **8** (1989) 157.
3. M. OBASA, H. NAKAMURA, M. TAKASAKA, T. KATO and M. NAGASAWA, *Polym. J.* **25** (1993) 301.
4. C. C. M. MA, L. T. HSIUE, W. G. WU and W. L. LIU, *J. Appl. Polym. Sci.* **39** (1990) 1399.
5. J. S. CHUNG and P. CEBE, *Polymer* **33** (1992) 2312.
6. *Idem., ibid.* **33** (1992) 2325.
7. N. A. MEHL and L. REBENFELD, *Polym. Eng. Sci.* **32** (1992) 1451.
8. C. HOU, B. ZHAO, J. YANG, Z. YU and Q. WU, *J. Appl. Polym. Sci.* **56** (1995) 581.
9. J. P. JOG and V. M. NADKARNI, *ibid.* **30** (1985) 997.
10. L. C. LOPEZ and G. L. WILKES, *Polymer* **29** (1988) 106.
11. *Idem., ibid.* **30** (1989) 882.
12. D. R. BUDGELL and M. DAY, *Polym. Eng. Sci.* **31** (1991) 1271.
13. V. L. SHINGANKULI, J. P. JOG and V. M. NADKARNI, *J. Appl. Polym. Sci.* **36** (1988) 335.
14. S. X. LU, P. CEBE and M. CAPEL, *Macromolecules* **30** (1997) 6243.
15. C. AUER, G. KALINKA, TH. KRAUSE and G. HINRICHSEN, *J. Appl. Polym. Sci.* **51** (1994) 407.
16. L. YE, T. SCHEURING and K. FRIEDRICH, *J. Mater. Sci.* **30** (1995) 4761.
17. J. S. JANG and H. S. KIM, *J. Appl. Polym. Sci.* **60** (1996) 2297.
18. H. J. PARK and B. C. CHUN, *Polym. Bull.* **37** (1996) 103.
19. T. H. CHEN and A. C. SU, *Polymer* **34** (1993) 4826.
20. V. M. NADKARNI and J. P. JOG, *J. Appl. Polym. Sci.* **32** (1986) 5817.

21. M.-F. CHEUNG, A. GOLOVOY, H. K. PLUMMER and H. V. OENE, *Polymer* **31** (1990) 2299.
22. M.-F. CHEUNG, A. GOLOVOY and H. V. OENE, *ibid.* **31** (1990) 2307.
23. M.-F. CHEUNG, A. GOLOVOY, V. E. MINDROIU, H. K. PLUMMER and H. V. OENE, *ibid.* **34** (1993) 3809.
24. S. AKHTAR and J. L. WHITE, *Polym. Eng. Sci.* **32** (1992) 690.
25. L. I. MINKOVA, M. PACI, M. PRACELLA and P. L. MAGAGNINI, *ibid.* **32** (1992) 57.
26. L. I. MINKOVA and P. L. MAGAGNINI, *Polymer* **36** (1995) 2059.

Received 28 January
and accepted 25 August 1999